Pure appl. geophys. 160 (2003) 429–438
0033–4553/03/020429–10



Pure and Applied Geophysics

# Three-dimensional Simulations of the Mean Air Transport During the 1997 Forest Fires in Kalimantan, Indonesia Using a Mesoscale Numerical Model

ORBITA ROSWINTIARTI[1] and SETHU RAMAN[1]

*Abstract* — This paper describes the meteorological processes responsible for the mean transport of air pollutants during the ENSO-related forest fires in Kalimantan, Indonesia from 00 UTC 21 September to 00 UTC 25 September, 1997. The Fifth Generation of the Pennsylvania State University-National Center for Atmospheric Research (PSU-NCAR) Mesoscale Model (MM5) is used to simulate three-dimensional winds at 6-hourly intervals. A nonhydrostatic version of the model is run using two nested grids with horizontal resolutions of 45 km and 15 km. From the simulated wind fields, the backward and forward trajectories of the air parcel are investigated using the Vis5D model.

The results indicate that the large-scale subsidence over Indonesia, the southwest monsoon low-level flows (2–8 m $s^{-1}$), and the shallow planetary boundary layer height (400–800 m) play a key role in the transport of air pollutants from Kalimantan to Malaysia, Singapore and Brunei.

**Key words:** Air quality, tropics, ENSO, long range transport, atmospheric boundary layer.

## *1. Introduction*

El Niño/Southern Oscillation (ENSO) is one of the most prominent and important phenomenon in the tropical ocean-atmosphere system at the interannual time scale (with a range of 2 to 7 years). The oceanic component, El Niño, is associated with the anomalous warm sea-surface temperature (SST) in the eastern-central tropical Pacific Ocean. The atmospheric component, Southern Oscillation, is related to the strength of the zonal Walker circulation over the Pacific region, i.e., the difference in surface pressure between the southeast tropical Pacific and the Indonesian-Australian regions. During the ENSO events, the eastward shift of deep convection from the Indonesian-Australian regions, which manifests as low Southern Oscillation Index (SOI), often leads to abnormally dry conditions over Indonesia (ROPELEWSKI and HALPERT, 1987). Many studies have also documented that the ENSO event is linked to a weakening of the Asia-Australia monsoon (WEBSTER and YANG, 1992).

[1] Department of Marine, Earth and Atmospheric Sciences, North Carolina State University, Raleigh, North Carolina 27695-8208, U.S.A.

In the 1997/98 ENSO event, drought conditions in Indonesia that persisted from June 1997 to May 1998 resulted in large-scale forest fires, particularly in Kalimantan and Sumatera Islands. It was reported that 3 million hectares of the forests were burned in Kalimantan and 1.5 million hectares in Sumatera. The associated smoke and haze that blanketed the neighboring countries of Malaysia, Singapore, and Brunei had substantial impacts on human life and economic development in the region.

The objective of this study is to characterize the wind circulations responsible for the transport of air pollutants during forest fires in Kalimantan in September, 1997. The Defense Meteorological Satellite Program (DMSP) detected numerous fires over east and south Kalimantan on 21 September, 1997 (Fig. 1a). Figure 1b displays the associated smoke distributions observed from the Total Ozone Mapping Spectrometer (TOMS) aerosol data. It is shown that the smoke coverage with aerosol indices $\geq 3.5$ spreads towards the neighboring countries of Malaysia, Singapore and Brunei. In this study, the Fifth Generation of the Pennsylvania State University-National Center for Atmospheric Research (PSU-NCAR) Mesoscale Model, known as MM5, is used to simulate the three-dimensional winds and the planetary boundary layer from 00 UTC, 21 September to 00 UTC 25 September, 1997. The backward and forward air mass trajectories determined from the simulated winds are examined to investigate the likely path of the mean air pollutants. The ability to anticipate the interactions between synoptic and regional meteorological processes during ENSO events in Indonesia, and improved predictions associated with the long-range transport of aerosols and pollutants would lead to better management decisions at the early stages of forest fire for future episodes.

This paper is arranged as follows: a brief description of the MM5 and the experimental design are described in section 2. Section 3 presents the model results and trajectory analyses. Conclusions of the study are given in section 4.

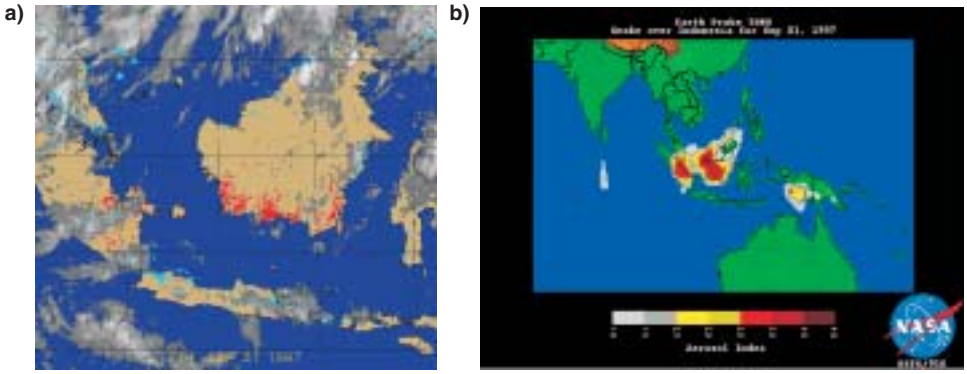


Figure 1
a) Forest fires (hotspots) in Kalimantan, Indonesia during the 1997/98 ENSO detected by the Defense Meteorological Satellite Program (DMSP) and b) associated smoke distributions observed by the Total Ozone Mapping Spectrometer (TOMS) aerosol data for 21 September, 1997.

## 2. Description of the Model and Experimental Design

The numerical model used in this study is a nonhydrostatic version of the MM5 (DUDHIA, 1993; GRELL *et al.*, 1995). The model used here has 21 $\sigma$ levels in the vertical (1.0, 0.999, 0.993, 0.971, 0.916, 0.888, 0.832, 0.777, 0.721, 0.666, 0.610, 0.499, 0.444, 0.388, 0.333, 0.277, 0.222, 0.166, 0.111, 0.055, 0.0) between surface and 100 hPa.

A simple-ice scheme (DUDHIA, 1989) is used for the nonconvective precipitation scheme. This scheme treats the microphysical processes of ice and snow identically to most other cloud-resolving models, except it does not include supercooled water and unmelted snow. The convective precipitation is parameterized using a Kuo-Anthes scheme (KUO, 1974; ANTHES, 1977). In this scheme, the amounts and the vertical distributions of the latent heat released and the sensible heat transported by the deep cumulus clouds are expressed solely in terms of the temperature difference between the environment and the convergence of moisture produced by the large-scale flow.

In the simulations the Blackadar high-resolution model (BLACKADAR, 1979; ZHANG and ANTHES, 1982) is used for planetary boundary layer physics. A simple radiative cooling model is used for the atmospheric radiation processes.

Figure 2 shows the model simulation domains in the Coarse-Grid Mesh (CGM) and Fine-Grid Mesh (FGM) which cover outer (15.5°N–15.3°S; 86.9°E–142.8°E) and inner regions (10.5°N–9.9°S; 105.0°E–124.7°E), respectively. The corresponding horizontal resolutions for the CGM and FGM are 45 km and 15 km, respectively. Thus there are $(79 \times 140)$ and $(159 \times 148)$ grid points for the CGM and FGM domains.

The European Centre for Medium-Range Weather Forecasts (ECMWF) analysis data with $2.5° \times 2.5°$ resolution at 15 pressure levels on 00 UTC 21 September, 1997 are used to specify the initial conditions. Figures 3a–b show the analyzed streamlines and wind speeds at 850 hPa and mean sea-level pressure (MSLP) for 00 UTC 21 September, 1997. The weak southwest monsoonal flows can be clearly seen in Figure 3a where the low-level easterly winds over northern Australia (with magnitudes between 2 and 8 m $s^{-1}$) curve as the southerly/southwesterly winds over Indonesia. These features are caused by a weak mean sea level pressure (MSLP) gradient between northern Australia and Southern Asia (Fig. 3b).

## 3. Model Results

### a. Streamlines and Wind Speeds

Figures 4a–b display the analyzed and day-1 simulated streamlines and wind speeds at 850 hPa over the CGM domain for 00 UTC 22 September, 1997. The model simulates the main features of the southwest monsoon flows reasonably well.

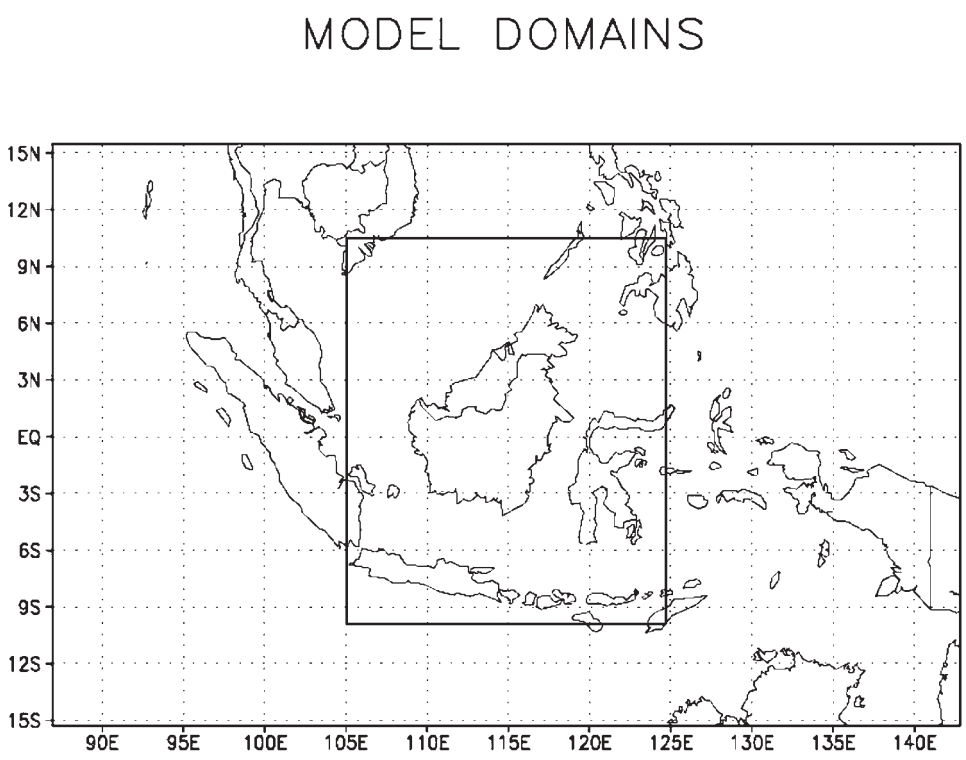


Figure 2
Model domains in the Coarse-Mesh Grid (CGM) and Fine-Mesh Grid (FGM) for the simulations.

These features include the easterly winds over the southeastern Indian Ocean and the cross-equatorial flows characterized by the deflected southeasterly winds into the southwesterly winds over the equator. Simulated wind speeds are also in the same range as the analyzed winds. However, high-pressure systems located over Philippines and the South Chine Sea to the west of Brunei are not simulated well.

Figures 4c–d display the analyzed and day-2 simulated streamlines and wind speeds at 850 hPa over the CGM domain for 00 UTC 23 September, 1997. The model simulates stronger easterly winds over the southeastern Indian Ocean and weaker southwesterly winds over the western Pacific Ocean. Distributions of winds are in close agreement with the analysis. However, the high-pressure system near the west coast of Brunei is missing in the simulation and wind speeds over the eastern part of Indonesia are not accurately simulated. Figures 5a–d show the analyzed and day-1 and day-2 simulated streamlines and wind speeds at 850 hPa over the FGM domain. A small improvement in the simulation of wind directions and wind speeds is gained as the resolution of the model increases. However, further analyses will focus on the coarse grid domain because of the transport over a larger area.

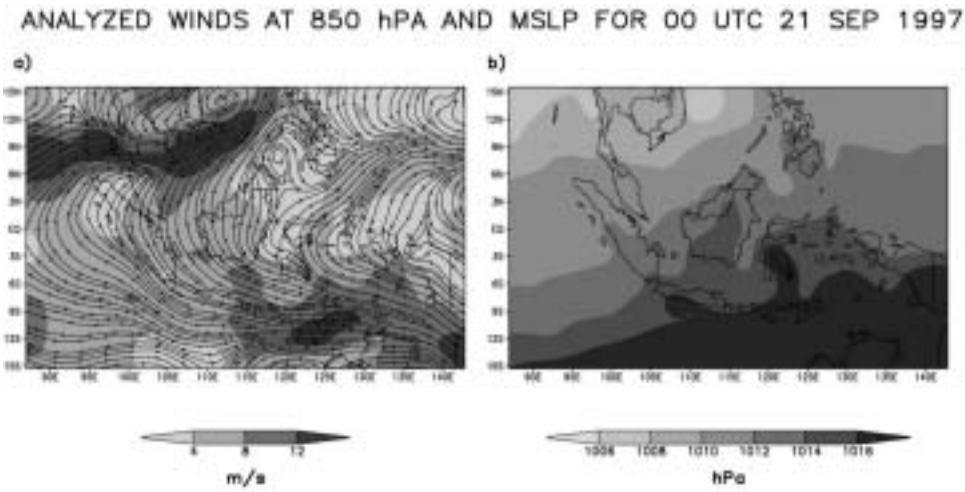


Figure 3
a) Analyzed streamlines and wind speeds at 850 hPa and b) mean surface pressure (MSLP) for 00 UTC 21 September, 1997 over the CGM domain as initial conditions.

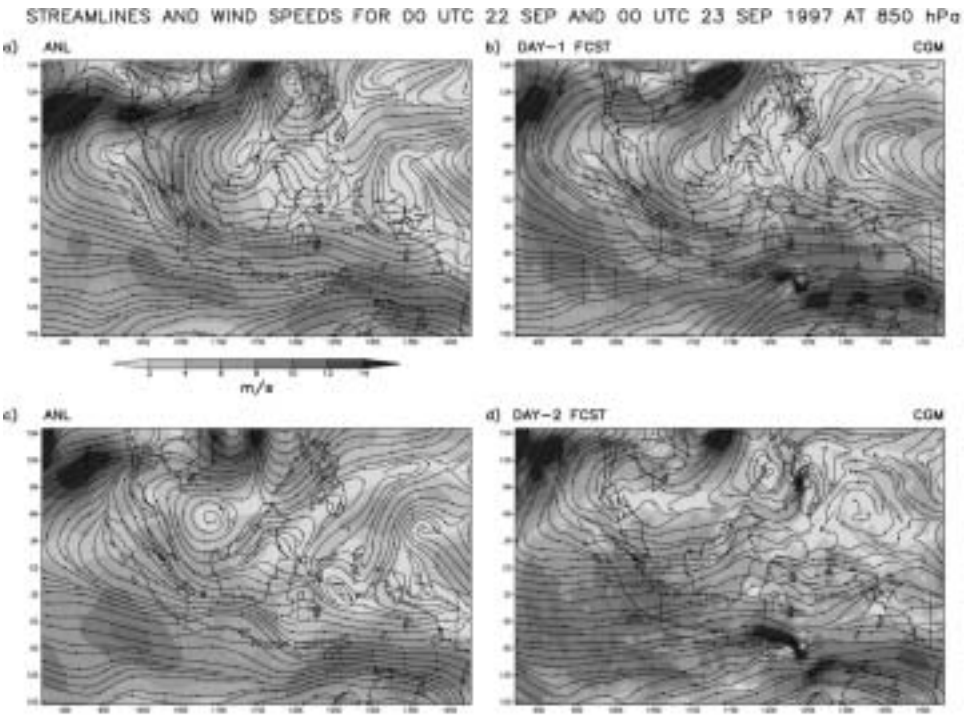


Figure 4
Analyzed and simulated streamlines and wind speeds at 850 hPa for 00 UTC 22 September, 1997 (a and b) and 00 UTC 23 September, 1997 (c and d) for the CGM domain.

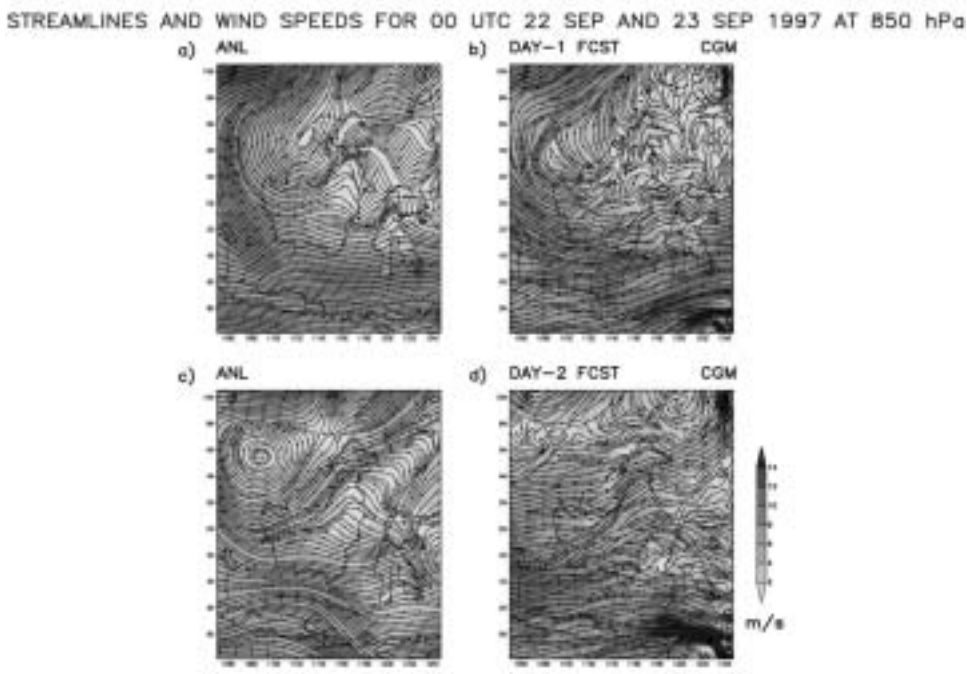


Figure 5
As in Figure 4, except for the FGM domain.

Figures 6a–b display the analyzed and day-3 simulated streamlines and wind speeds at 850 hPa over the CGM domain for 00 UTC 24 September, 1997. The low-level flow analysis indicates that easterly winds particularly over Kalimantan, Java, and Sumatera become the southeasterly winds and the simulated winds are in general agreement with the analyzed winds. Figures 6c–d display the analyzed and day-4 simulated streamlines and wind speeds at 850 hPa over the CGM domain for 00 UTC 25 September, 1997. Although the mean circulations can be simulated reasonably, the wind speeds over the southeastern Indian Ocean are slightly overestimated, while those over the western Pacific are underestimated. The forecast skills given by mean, bias, root-mean-square error, and correlation coefficient between the analyzed and simulated winds for the CGM are given in Table 1.

Figures 7a–d show the simulated planetary boundary layer heights for 06 UTC 21 September, 1997, 12 UTC 21 September, 1997, 18 UTC 21 September, 1997, and 00 UTC 22 September, 1997. It is clear that the simulated planetary boundary layer heights vary with time and space. However, under the influence of large-scale subsidence and low-level divergence the simulated boundary layer height is shallow with values less than 1200 m evn over land in locations such as Brunei. This condition leads to the entrapment of pollutants in the boundary layer.

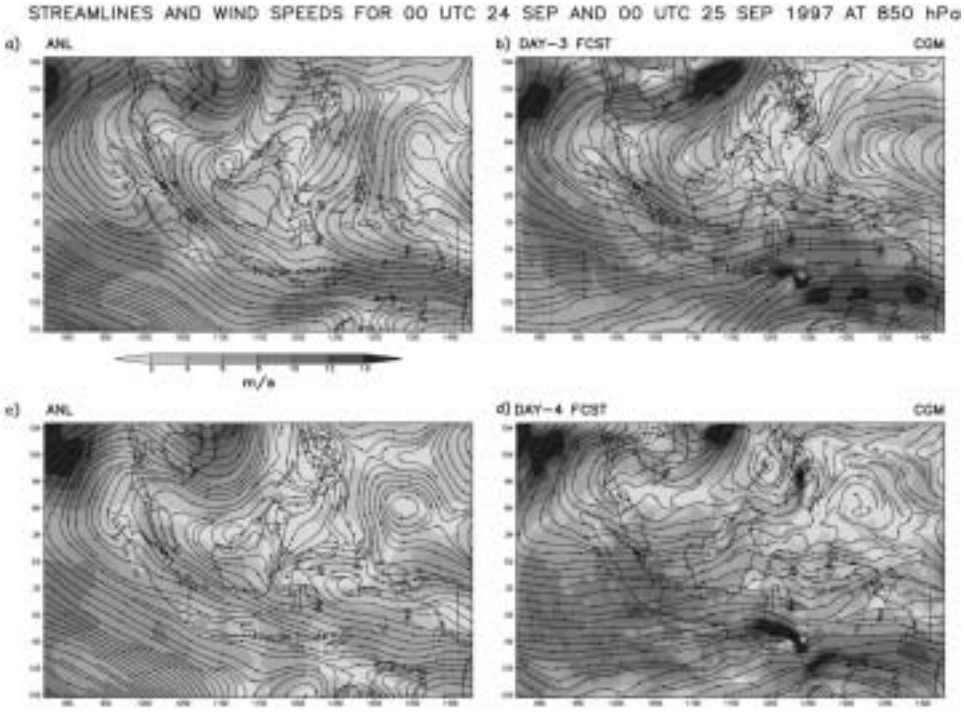


Figure 6
Analyzed and simulated streamlines and wind speeds at 850 hPa for 00 UTC 24 September, 1997 (a and b) and 00 UTC 25 September, 1997 (c and d) for the CGM domain.

Table 1

*Forecast skill statistics for the CGM domain*

| Date | Var. | Mean (m $s^{-1}$) | | BIAS (m $s^{-1}$) | RMSE (m $s^{-1}$) | CORR |
|---|---|---|---|---|---|---|
| | | ANL | MM5 | | | |
| 00 UTC | U | −3.1 | −2.2 | 0.9 | 2.9 | 0.89 |
| 22 Sep. 97 | V | 1.3 | 1.3 | 0.0 | 2.1 | 0.77 |
| 00 UTC | U | −3.8 | −2.2 | 1.4 | 3.2 | 0.85 |
| 23 Sep. 97 | V | 0.6 | 1.1 | 0.5 | 2.5 | 0.67 |
| 00 UTC | U | −4.2 | −2.2 | 2.0 | 3.5 | 0.82 |
| 24 Sep. 97 | V | 1.3 | 1.9 | 0.6 | 2.9 | 0.54 |
| 00 UTC | U | −3.5 | −1.4 | 1.9 | 3.4 | 0.83 |
| 25 Sep. 97 | V | 0.9 | 1.5 | 0.6 | 2.7 | 0.66 |

### *b. Trajectories Analysis*

Since a pollutant spreads out both horizontally and vertically due to dispersion, a realistic representation of the mean transport can only be obtained from an ensemble

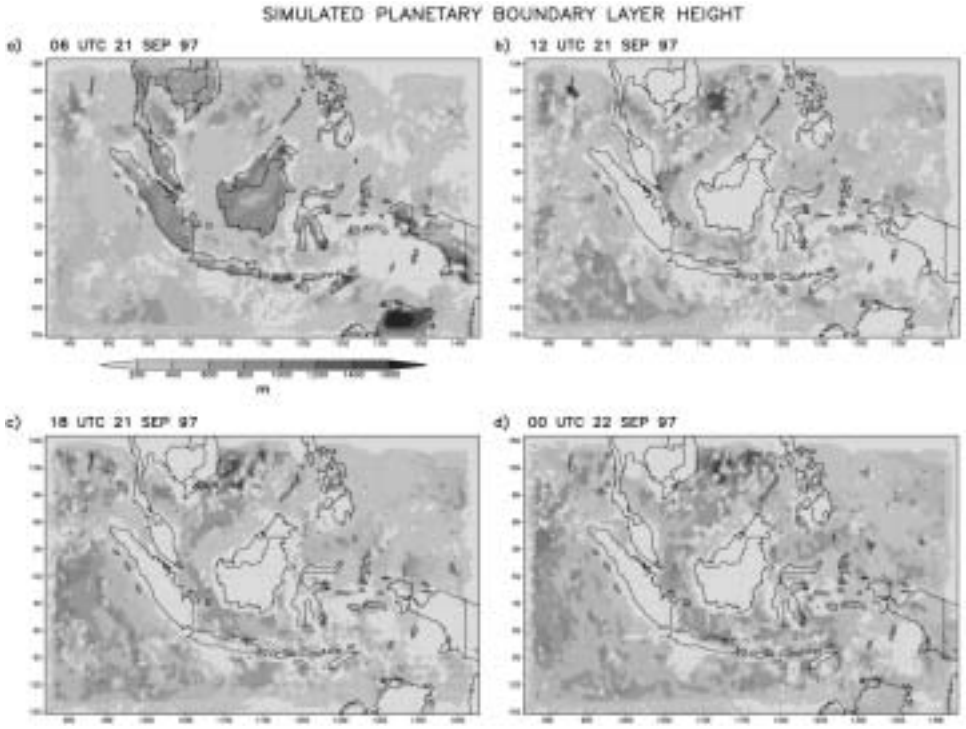


Figure 7
Simulated planetary boundary layer heights for a) 06 UTC 21 September, 1997, b) 12 UTC 21 September, 1997, c) 18 UTC 21 September, 1997, and d) 00 UTC 22 September, 1997 for the CGM domain.

of various trajectory pathways. Trajectories are examined between 900 hPa (~1 km) and 850 hPa (~1.5 km). These altitudes are chosen to represent average plume rises and to examine the coupling of flows in the lower boundary layer with flows at higher altitudes.

Figure 8 displays the backward trajectories ending in Malaysia and Singapore at 00 UTC 25 September, 1997 at 900 hPa. Backward trajectories are used to identify the source of air masses classified as polluted air. In general, air parcels arrive in Malaysia and Singapore at 900 hPa originating from east Kalimantan at 800 hPa. Because of persistently low-level easterly winds (with amplitude 6–7 m $s^{-1}$), transport from 116°E to 102°E takes place in only four days. Figure 9 illustrates the backward trajectories terminating in Malaysia and Singapore at 00 UTC 25 September, 1997 at 850 hPa. Air masses from Sarawak and the South China Sea at 800 hPa arrive in Malaysia at 850 hPa. Meanwhile, plumes from east Kalimantan make their way to Singapore.

These simulations illustrate that the long-range transports involve the entire depth of the troposphere. Moreover, the large-scale subsidence and dry atmosphere associated with the 1997/98 ENSO event cause aerosols and pollutants in the upper troposphere to move downward rapidly to the surface.

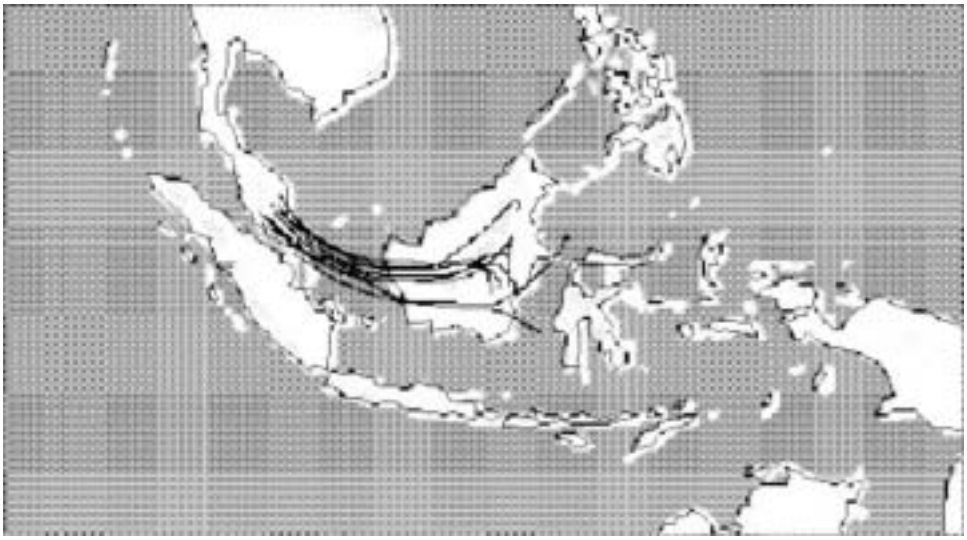

Figure 8
Backward trajectories terminating at 00 UTC 25 September, 1997 at 900 hPa in Malaysia and Singapore.

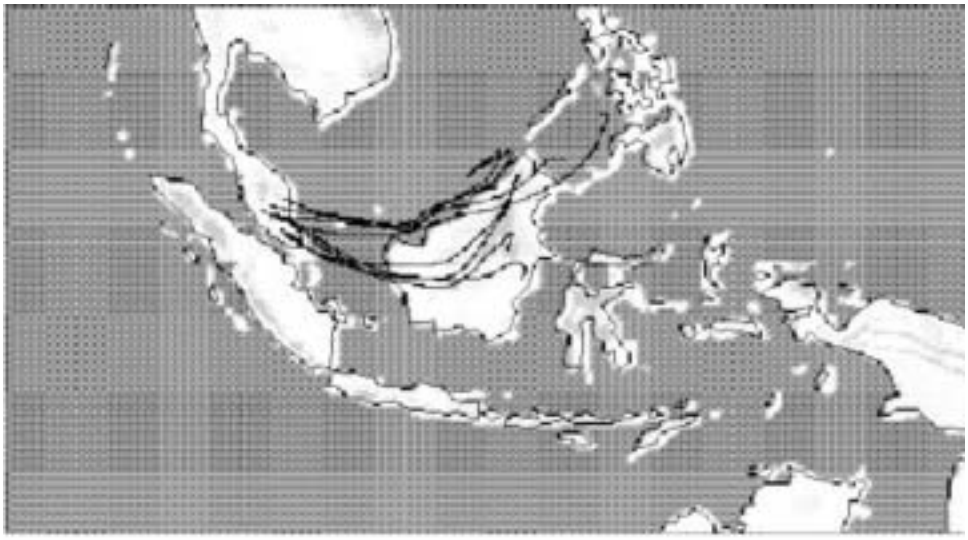

Figure 9
Backward trajectories terminating at 00 UTC 25 September, 1997 at 850 hPa in Malaysia and Singapore.

## *4. Conclusions*

Advection by synoptic-scale winds and entrainment into the boundary layer are the primary mechanisms responsible for transporting air pollutants and aerosols

during forest fires in Kalimantan between 00 UTC 21 September to 00 UTC 25 September, 1997. The MM5 model is able to simulate the general features of the transport. The winds in this region are generally easterly/southeasterly driven by the synoptic pressure gradient between the Indonesian-Australian regions and Southeast Asia. The transport of air masses is reasonably well coupled with mean flows through the lower and upper troposphere. Since there are large-scale subsidence and no precipitating clouds, there is no removal of aerosols through precipitation.

*Acknowledgements*

This work was supported by the Atmospheric Sciences Division, National Science Foundation under grant ATM–9632390 and ATM–0080088.

## References

ANTHES, R. A. (1977), *A Cumulus Parameterization Scheme Utilizing a One-dimensional Cloud Model*, Mon. Wea. Rev. *105*, 270–286.

BLACKADAR, A. K., *High resolution models of the planetary boundary layer*. In *Advances in Environmental Science and Engineering* (J. Pfafflin and E. Ziegler, eds.) vol. 1, (Gordon and Breach, 1979) pp. 50–85.

DUDHIA, J. (1989), *Numerical Study of Convection Observed During the Winter Monsoon Experiment Using a Mesoscale Two-dimensional Model*, J. Atmos. Sci. *46*, 3077–3107.

DUDHIA, Y. (1993), *A Nonhydrostatic Version of the Penn State-NCAR Mesoscale Model: Validation Tests and Simulations of an Atlantic Cyclone and Cold Front*, Mon. Wea. Rev. *121*, 1493–1513.

GRELL, G. A., DUDHIA, J., and STAUFFER, R. D. (1995), *A Description of the Fifth-generation Penn State/NCAR Mesoscale Model (MM5)*, NCAR Tech. Note TN-398 + STR, 122 pp. [Available from UCAR Communications, P. O. Box 3000, Boulder, CO 80307.]

KUO, H. L. (1974), *Further Studies of the Parameterization of the Influence of Cumulus Convection of Large-scale Flow*, J. Atmos. Sci. *31*, 1232–1240.

ROPELEWSKI, C. F. and HALPERT, M. S. (1987), *Global and Regional Scale Precipitation Patterns Associated with the El Niño/Southern Oscillation*, Mon. Wea. Rev. *115*, 1606–1624.

WEBSTER, P. J. and YANG, S. (1992), *Monsoon and ENSO: Selective Interactive Systems*, Quart. J. Roy. Meteor. Soc. *118*, 877–926.

ZHANG, D. and ANTHES, R. A. (1982), *A High-resolution Model of the Planetary Boundary Layer-Sensitivity Tests and Comparisons with SESAME-79 Data*, J. Appl. Meteor. *21*, 1954–1609.

(Received July 1, 2000, accepted May 26, 2001)